Electrical conductivity and equation-of-state study of warm dense copper: Measurements and quantum molecular dynamics calculations

Jean Clérouin,* Patrick Renaudin, Yann Laudernet, and Pierre Noiret
Département de Physique Théorique et Appliquée, CEA/DAM Île-de-France, Boîte Postale 12, 91680 Bruyères-le-Châtel Cedex, France

Michael P. Desjarlais
Pulsed Power Sciences Center, Sandia National Laboratories, Albuquerque, New Mexico 87185-1186, USA
(Received 6 September 2004; revised manuscript received 20 December 2004; published 23 February 2005)

Absolute measurements of the pressure and the electrical conductivity of expanded copper in the warm dense matter regime ($\rho=0.5-0.3$ g/cm^3 and 6000 K$<T<$30 000 K) are obtained in an isochoric plasma closed-vessel (EPI). Quantum molecular dynamics simulations are found to be in excellent agreement with the experimental results, allowing for a detailed interpretation of the optical conductivities. A shift in energy of the $4s\rightarrow 4p$ atomic line is explained by the rise of ionization with temperature.

DOI: 10.1103/PhysRevB.71.064203 PACS number(s): 52.25.−b, 52.65.−y, 52.50.−b, 52.70.−m

I. INTRODUCTION

Expanded liquid metals are a very important field of research because they are a privileged system to study the metal-nonmetal transition (MNM).[1] This transition occurs when a metal vaporizes into a low density atomic phase or when it is brought through the region of the critical point. Due to their low critical temperatures, metals such as cesium, rubidium, or mercury have been intensively studied for the MNM transition. In the case of transition metals such as copper, which have a high and imprecisely determined critical temperature (between 5000 and 10 000 K),[2,3] accurate experimental results are more difficult to obtain. Consequently, to avoid the liquid-gas coexistence region, experiments must be performed at high temperatures (typically $T>10\,000$ K) corresponding to pressures of order of 1 or 2 GPa. This regime which combines low density and high temperatures is of a great interest because two opposite behaviors are competing: a strong lowering of the electrical conductivity with decreasing density (MNM-like transition) and a thermal activation of the conductivity (ionization).

These two behaviors are illustrated in Fig. 1 where previous experimental data for the dc conductivity of copper, measured for different temperatures and densities are reported.[4] For $T=10\,000$ K, the experimental conductivities (filled triangles) are decreasing with the density with a power-law behavior and a minimum at a very low density ($\rho<0.1$ g/cm^3). At higher temperature ($T=30\,000$ K, filled circles), the conductivity versus density quickly saturates at higher values. These two behaviors are well reproduced by the quantum molecular dynamics (QMD) simulations we will describe later (open symbols). For a given density ($\rho=0.5$ g/cm^3 or $\rho=0.3$ g/cm^3) the enhancement of the dc conductivity with the temperature is clearly evident. It is a behavior characteristic of a semiconductor in contrast with a simple metal where the electrical conductivity diminishes with the temperature. The shaded area corresponds to the experimental domain accessible with the EPI facility ("Enceinte à Plasma Isochore"). This region is particularly interesting because it maps the transition from low density atomic vapor to the partially ionized plasma. Such a regime, also referred to as warm dense matter, is also characterized by strongly coupled ions and partially degenerate electrons.

The goal of this paper is to show, by a careful comparison with experimental data, that quantum molecular dynamics simulations are particularly well suited for describing this regime and are providing a consistent view of the system in terms of the equation of state (EOS) and the transport properties.

II. EXPERIMENTS

The experiments were conducted with the EPI facility, which has been described in detail in previous papers.[5–7]

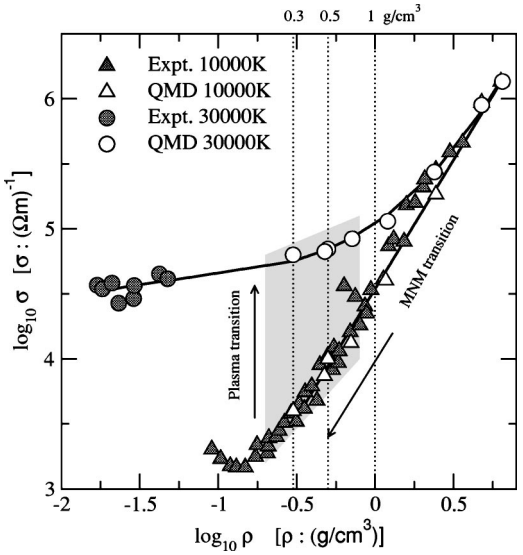

FIG. 1. dc conductivity of copper vs density for two temperatures $T=10\,000$ K (triangles) and $T=30\,000$ K (circles). Symbols in gray correspond to DeSilva and Katsouros' experiments (see Ref. 4), and open symbols to quantum molecular dynamics simulations. Black lines are shown to help identify the two regimes. The shaded area covers the experimental regime for the EPI facility.

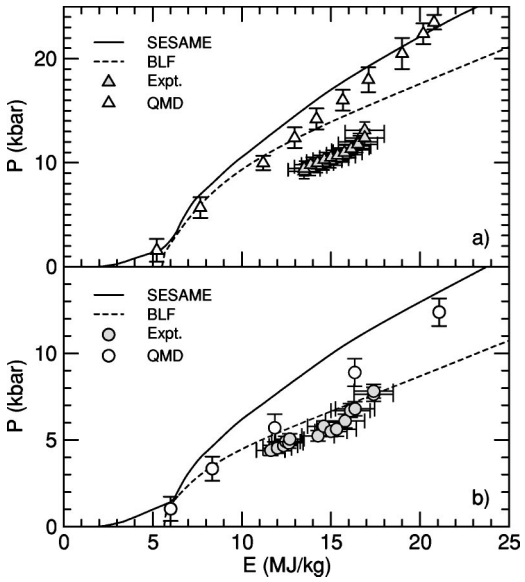

FIG. 2. Pressure vs energy. (a) $\rho=0.5\ \mathrm{g/cm^3}$ and (b) $\rho=0.3\ \mathrm{g/cm^3}$. Filled symbols in grey are EPI experiments and open symbols QMD simulations. Corresponding SESAME EOS (full line) and BLF EOS (dotted line).

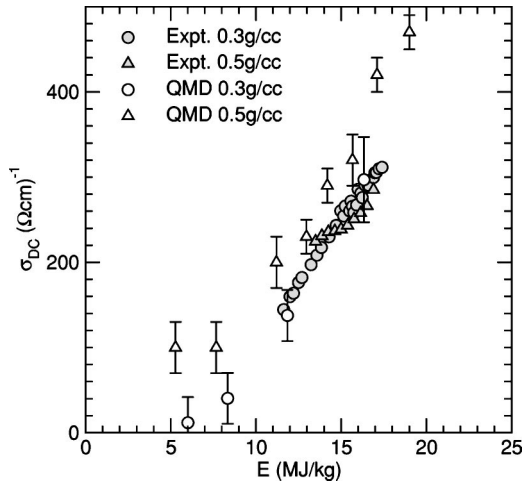

FIG. 3. dc conductivity σ_{dc} vs energy for two densities $\rho=0.5\ \mathrm{g/cm^3}$ and $\rho=0.3\ \mathrm{g/cm^3}$. Same symbols as in Fig. 2.

This facility allows absolute measurements of the energy, pressure, and conductivity without the help of any external models. The amount of matter in the chamber yields the exact density of the plasma which, due to the slowness of the discharge (250 μs) is almost homogeneous. The plasma heating is assumed to be done along an isochore. Two piezoelectrical sensors with 2 μs rise time are placed at each end of the sapphire tube to measure the pressure during the discharge. The sensors are acceleration compensated and allow one to measure a maximum pressure (0.7 GPa) lower than the plasma pressure. There is no contact between them and the plasma. A surface divider piston reduces by a factor of 4 the applied pressure and transmits it to the sensor. A dynamic and static calibration is performed before each experiment. A free-falling known mass is dropped onto a piston, creating a pressure pulse onto the sensor. By measuring the drop-mass velocity before and after the impact, the applied momentum on the sensor is deduced. The uncertainty in the drop mass after impact velocity measurements produces a 15% uncertainty in the pressure of the plasma. To measure the static coefficient, a well-defined force is applied to the sensor. The force is obtained by measuring the crushing of small copper cylinders. These two procedures lead to two different calibration coefficients which are equal to within 5%. The electrical conductivity is deduced from the time evolution of current and voltage. Note that all quantities are known versus the internal energy variation; to preserve the absolute character of our data we will show them this way (see Figs. 2 and 3). The uncertainties in the measurements of the conductivity are related to the accuracy of current and voltage measurements and are estimated at about 15%. The uncertainty in the internal energy variation is a little bit more complex to estimate, due to the ablation of the internal channel containing the plasma. When the energy is translated into temperature with an external model as for Fig. 1, such as a SESAME table,[8] our values of the dc conductivity are in agreement with DeSilva and Katsouros' previous measurements.[4]

III. QUANTUM MOLECULAR DYNAMICS SIMULATIONS

Quantum molecular dynamics simulations were generated with the QMD package VASP, developed at the Technical University of Vienna.[9] The projector augmented wave (PAW) potentials[10] were used for the ion-electron interaction, and exchange correlation terms were treated at the level of the generalized gradient approximation (GGA), in the Perdew and Wang parametrization.[11]

From the knowledge of the matrix elements, the optical conductivities (OC) are obtained with the Kubo-Greenwood (KG) formulation[12,13] (atomic units)

$$\sigma(\omega)=\frac{2\pi}{3\omega}\frac{1}{\Omega}\sum_{\boldsymbol{k}} W(\boldsymbol{k}) \sum_{n,m,\alpha} (f_n^{\boldsymbol{k}}-f_m^{\boldsymbol{k}})|\langle\psi_n|\nabla_\alpha|\psi_m^{\boldsymbol{k}}\rangle|^2 \times\delta(E_m^{\boldsymbol{k}}-E_n^{\boldsymbol{k}}-\hbar\omega), \quad (1)$$

where ω is the frequency, e is the electronic charge, ψ_n and E_n are the electronic eigenstates and eigenvalues for the electronic band n at a given $\boldsymbol{k}$ point in the Brillouin zone with the $W(\mathbf{k})$ $\boldsymbol{k}$ point weight using the Monkhorst-Pack scheme. f_n is the Fermi distribution function, and ∇_α is the velocity operator along each direction ($\alpha=x,y,z$). Here, the KG formulation is applied using the all electron PAW potential and does not require the correction term related to the nonlocality of the pseudopotential that would be needed if ultrasoft pseudopotentials were used.[10,14,15]

The δ function is resolved by using a Gaussian regularization.[14] The dc electrical conductivity σ_{dc} is obtained by extrapolating the low frequency optical conductivity to $\omega=0$. The eigenstates and eigenvalues are here the solutions of the Kohn-Sham equations and are thus computed within the local density approximation.

For copper, 10*d* electrons and 1*s* electron must be considered in the construction of the pseudopotential. Thus 11 electrons must be handled making simulations expensive. A

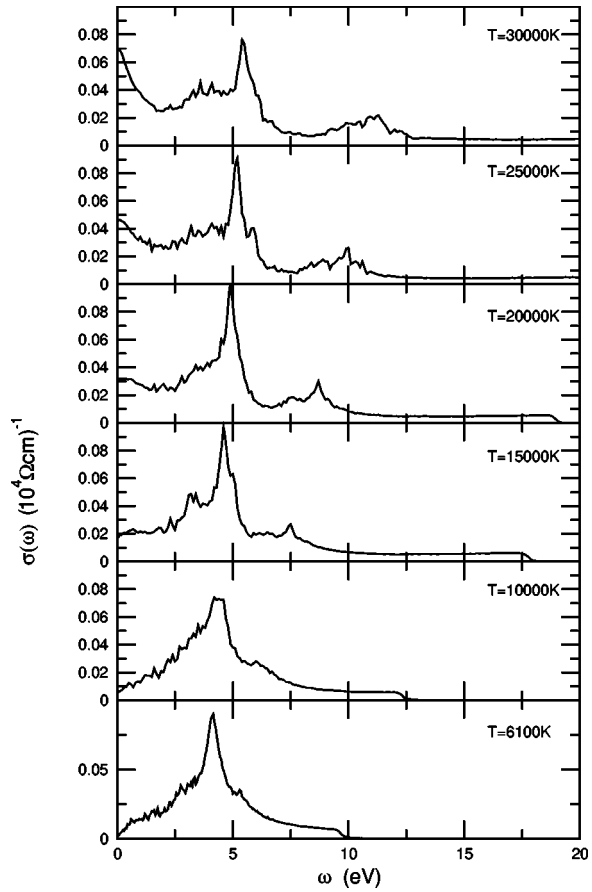

FIG. 4. Optical conductivity vs energy for different temperatures at 0.5 g/cm^3.

300 K fcc QMD simulation of the solid phase with 32 atoms sets the reference energy. All further energies are given relative to this reference energy. In accord with the experiments, two densities were explored 0.5 and 0.3 g/cm^3. Simulations were done at Γ point with 32 atoms for the highest density (0.5 g/cm^3) and with 20 atoms for the lowest one (0.3 g/cm^3). For each density, the ionic temperature was varied and the electronic temperature was set to the same value. The pressure was measured and the electrical conductivity was computed afterwards and averaged over 5–10 independent configurations extracted from the ionic trajectories, following the procedure discussed in preceding papers.[5,14,16] To increase the precision of the calculation of the conductivity,[17] a better 8-k points Brillouzin zone (BZ) sampling was used and more bands were included to satisfy the sum rule on conductivity [see Eq. (20) in Ref. 18]. For the lowest density with 20 ions the number of bands was increased from 170 to 900 at 6000 K and from 400 to 2000 at 30 000 K. The dc electrical conductivity computed for the reference case (ρ_0,300 K) yields 60×10^4 $(\Omega\ \mathrm{cm})^{-1}$ in excellent agreement with the experimental value of 57×10^4 $(\Omega\ \mathrm{cm})^{-1}$ found in handbooks.[19]

IV. RESULTS

The experimental pressures are reported in Fig. 2 for the two densities considered (filled symbols). For the highest density [Fig. 2(a)] experimental pressures are below the SESAME 3332 EOS and the Russian EOS BLF.[20] The QMD pressures (open symbols) are higher than the experimental pressures. For the lowest density [Fig. 2(b)] the BLF EOS reproduces accurately the experimental data. QMD simulations are also in excellent agreement with data in the low energy region ($E<20$ MJ/kg). It is worth noting that at higher energies, the QMD points join with the SESAME EOS. For a given energy, the increase of the density leads to a corresponding increase in the pressure, which is satisfactory.

TABLE I. dc electrical conductivity σ and estimated number of free electrons N_e from the fits to the optical conductivities at $\rho=0.5$ g/cm^3.

T (K)	σ_{dc} $(\Omega\ \mathrm{cm})^{-1}$	N_e
30000	700	0.73
25000	540	0.56
20000	310	0.32
15000	200	0.21
10000	100	0.10

In Fig. 3 the experimental electrical conductivities versus energy are compared for both densities. The striking feature is that now no density dependency for the dc conductivity is observed in contrast with Likalter's prediction[2] of 700 $(\Omega\ \mathrm{cm})^{-1}$ at 0.5 g/cm^3 and 130 $(\Omega\ \mathrm{cm})^{-1}$ at 0.3 g/cm^3 for a temperature of 7600 K corresponding to an energy of about 10.5 MJ/kg. Values for $\rho=0.5$ g/cm^3 (gray triangles) and $\rho=0.3$ g/cm^3 (gray circles) are indistinguishable, which corresponds to a plateau in Fig. 1. Conversely, a clear enhancement of the electrical conductivity with energy (and temperature) appears well reproduced by the QMD simulations.

V. OPTICAL CONDUCTIVITIES

The excellent agreement between experiments and simulations observed for the dc conductivities and simultaneously good agreement for the EOS motivates further theoretical interpretation of the simulations. We proceed by considering the whole optical conductivity as given by the KG formula (1). We have shown that for aluminum the OC was perfectly described by a Drude behavior in the liquid phase, but was dominated by atomic transitions in the expanded regime.[5,14,16] This is also clearly evidenced for copper by the evolution of the OC with temperature as shown in Fig. 4. Three conclusions can be drawn from the inspection of Fig. 4. First, the zero-frequency value of $\sigma(\omega)$ which yields the dc electrical conductivity increases with temperature. Second, we observe a well defined peak at low temperature which moves towards higher energies with temperature. By comparing with isolated atomic lines this peak can be identified as the $4s\rightarrow4p$ transition. Third, a small peak, at about 6 eV at low temperature, is also seen to move to higher energies at 30 000 K. The interpretation of such a spectra can

no longer be done by the mean of the sole Drude model. As quoted by authors doing experiments with ultra-short lasers[21,22] the OC in this regime must be computed using both the Drude model and the atomic polarizability. This is particularly clear for the 30 000 K case where the spectrum can be considered as the superposition of a Drude central peak with a few isolated peaks, as already observed in the very dilute regime for aluminum.[14] We have thus adopted a formulation for the dielectric function

$$\epsilon(\omega) = 1 + 4\pi n_a \alpha(\omega) + \frac{4\pi i \sigma(\omega)}{\omega} \tag{2}$$

in which n_a is the number of atoms, $\alpha(\omega)$ is the polarizability, and $\sigma(\omega) = N_e e^2 \tau_D / m_e \times 1/(1 - i\omega\tau)$ is the usual Drude conductivity.

The atomic polarizability can be described by a simple Lorentz model, by summing over a finite number of oscillators of frequencies ω_i, and relaxation times τ_{at}^j. The whole shape of $\sigma(\omega)$ is easily fitted for the highest temperature (30 000 K) where a clear Drude contribution can be identified unambiguously. The inputs for the fit are the dc conductivity and the frequencies of a few dominant peaks. The relaxation times (τ_D and τ_{at}^j) are then adjusted by a mean square minimization algorithm. For the 30 000 K case, this procedure yields a relaxation time of 7.18×10^{-16} s and a number of free electrons of 0.73 per copper atom. At lower temperature, this procedure would lead to too small relaxation times because the zero frequency peak is vanishing and hidden by some low frequency contributions forming a shoulder at about $\simeq 2$ eV. In order to estimate the Drude part of the OC we have supposed that, at the zeroth order, the Drude relaxation time τ_D was fixed to its high temperature value. Doing so we are able to estimate the Drude contribution even for the lowest temperature and we get a number of conduction electrons increasing with the temperature, which is satisfactory (see Table I). Since we generally expect the collision time to increase somewhat with energy over this temperature range, this assumption of a constant collision time will tend to underestimate the number of free electrons at lower densities. The shift towards high energies of the main peak ($4s \rightarrow 4p$) with temperature is interpreted as a consequence of the increasing number of free electrons. The frequency of this transition, located at 3.8 eV for atomic copper, shifts to 5.5 eV in the singly ionized atom. The density functional theory (DFT), which considers statistically populated levels, realizes a continuous transition from the atomic to the singly ionized state and, hence, a continuous shift, as also observed for expanded aluminum.[23] This shift in the frequency can be traced back to the substantial change of the density of state with pressure and temperature as explained in a previous paper.[24] The case of the small peak, which moves from 5.2 to about 12 eV is more complex, but appears to be related to the $3d \rightarrow 4p$ transition.

VI. CONCLUSION

To summarize, we have obtained experimental results for the pressure and electrical conductivity of expanded copper for two densities $\rho = 0.5$ g/cm^3 and $\rho = 0.3$ g/cm^3 and temperatures ranging from 6000 to 30 000 K. These results are fairly well reproduced by quantum molecular dynamics simulations. In this regime, close to the saturation curve, the experimental pressures are in better agreement with the BLF EOS for both densities. At higher temperatures, the QMD simulations approach the Sesame result. The behavior of the electrical conductivity shows a weak dependance with the density and a more pronounced dependance with the temperature, confirmed by QMD simulations. The simulations are also used to interpret the optical conductivities, and the shift of the main atomic transition $4s \rightarrow 4p$ towards high energy.

ACKNOWLEDGMENTS

Sandia is a multiprogram laboratory operated by Sandia Corporation, a Lockheed Martin Company for the United States Department of Energy's National Nuclear Security Administration under Contract No. DE-AC04-94AL85000. This work was performed under the auspices of an agreement between CEA/DAM and NNSA/DP on cooperation on fundamental science. B. Loffredo and M. Sonnaert are acknowledged for their experimental support and also S. Mazevet for discussions.

*Electronic address: jean.clerouin@cea.fr

[1] F. Hensel and W. W. Warren, *Fluid Metals* (Princeton University Press, Princeton, NJ, 1999).
[2] A. A. Likalter, J. Phys.: Condens. Matter **4**, 10 125 (1992).
[3] A. A. Likalter, Phys. Rev. B **53**, 4386 (1996).
[4] A. W. De Silva and J. D. Katsouros, Phys. Rev. E **57**, 5945 (1998).
[5] V. Recoules, P. Renaudin, J. Clérouin, P. Noiret, and G. Zérah, Phys. Rev. E **66**, 056 412 (2002).
[6] P. Renaudin, C. Blancard, G. Faussurier, and P. Noiret, Phys. Rev. Lett. **88**, 215 001 (2002).
[7] P. Renaudin, C. Blancard, J. Clérouin, G. Faussurier, P. Noiret, and V. Recoules, Phys. Rev. Lett. **91**, 075 002 (2003).
[8] S. P. Lyon and J. D. Johnson, SESAME: The Los Alamos National Laboratory Equation of State Database, Report No. LA-UR-92-3407 (Group T-1, 1992).
[9] G. Kresse and J. Hafner, Phys. Rev. B **47**, R558 (1993).
[10] G. Kresse and D. Joubert, Phys. Rev. B **59**, 1758 (1999).
[11] J. P. Perdew, *Electronic Structure of Solids* (Akademie Verlag, Berlin, 1991).
[12] R. Kubo, J. Phys. Soc. Jpn. **12**, 570 (1957).
[13] D. A. Greenwood, Proc. Phys. Soc. Jpn. **71**, 585 (1958).
[14] M. P. Desjarlais, J. D. Kress, and L. A. Collins, Phys. Rev. E **66**, 025 401(R) (2002).
[15] P. E. Blochl, Phys. Rev. B **50**, 17 953 (1994).
[16] V. Recoules, J. Clérouin, P. Renaudin, P. Noiret, and G. Zérah, J.

Phys. A **36**, 6033 (2003).
[17] P. L. Silvestrelli, A. Alavi, and M. Parrinello, Phys. Rev. B **55**, 15 515 (1997).
[18] L. A. Collins, S. R. Bickham, J. D. Kress, S. Mazevet, T. J. Lenosky, N. J. Troullier, and W. Windl, Phys. Rev. B **63**, 184 110 (2001).
[19] *CRC Handbook of Chemistry and Physics*, edited by R. C. Weast, M. J. Astle, and W. H. Beyer (CRC Press, Cleveland, 1986-1987), 67th ed.
[20] A. V. Bushman, I. V. Lomonosov, and V. E. Fortov, *Equation of State of Metals at High Energy Densities* (Institute of Chemical physics, Russian Academy of Sciences, Chernogolovka, 1992) (in Russian).
[21] H. Yoneda, H. Morikami, K. I. Ueda, and R. M. More, Phys. Rev. Lett. **91**, 075 004 (2003).
[22] K. Widmann, T. Ao, M. E. Foord, D. F. Price, A. D. Ellis, P. T. Springer, and A. Ng, Phys. Rev. Lett. **92**, 125 002 (2004).
[23] S. Mazevet, M. P. Desjarlais, L. A. Collins, J. D. Kress, and N. H. Magee, Phys. Rev. E **71**, 016409 (2005).
[24] Y. Laudernet, J. Clérouin, and S. Mazevet, Phys. Rev. B **70**, 165 108 (2004).